

Analysis of the semileptonic $B_c \rightarrow D_s^* \mu^+ \mu^-$ decay mode in the effective field theory approach

Ajay Kumar Yadav^{1,*}, Manas Kumar Mohapatra^{2,**}, and Suchismita Sahoo^{1,***}

¹Department of Physics, Central University of Karnataka, Kalaburagi-585367, India

²School of Physics, University of Hyderabad, Hyderabad-500046, India

Abstract. Discrepancies have been noted between experimental measurements and Standard Model predictions for various observables related to the $B \rightarrow (K, K^*, \phi) ll$ processes. Recently, the Belle-II Collaboration observed a 2.8σ deviation from Standard Model predictions in the branching ratio of the $B \rightarrow K \nu_l \bar{\nu}_l$ decay mode. In this context, we investigate the exclusive semileptonic $B_c \rightarrow D_s^* \mu^+ \mu^-$ decay mode, mediated by $b \rightarrow s$ quark level transition, using Effective Field Theory formalism. We perform a global fit to the new parameters using existing experimental data on $b \rightarrow s \mu^+ \mu^-$. We then estimate the branching ratio and other observables such as forward-backward asymmetry, lepton polarisation asymmetry, and the lepton non-universality parameter of the $B_c \rightarrow D_s^* \mu^+ \mu^-$ process. Although this process has not yet been detected experimentally, we offer predictions and discuss the observables for $B_c \rightarrow D_s^* \mu^+ \mu^-$ in both the Standard Model and potential new physics scenarios.

1 Introduction

The Standard Model (SM) is a remarkable framework for understanding fundamental particles and their interactions. However, it does not provide a complete picture of the Universe, such as the matter-antimatter asymmetry, gravitational interaction, neutrino mass mechanisms, and the nature of dark matter and dark energy. Due to the disagreements between the SM predictions and experimental observations, the $b \rightarrow s l l$ transition of B meson decays has been a hot topic of discussion. This transition involves flavor-changing neutral currents, which are not allowed at the tree level in the SM and these currents are further suppressed by elements of the Cabibbo–Kobayashi–Maskawa (CKM) matrix, making them highly sensitive to small effects from new physics. Recently, there have been advancements in the field of physics with the simultaneous measurements of R_K and R_{K^*} with q^2 values [0.1 – 1.1] and as well as [1.1 – 6], demonstrating excellent agreement with SM predictions at 0.2σ [1, 2]. However, there are still discrepancies in other observables, such as the branching fraction $BR(B \rightarrow \phi ll)$ [3]. Additionally, the CMS experiment recently observed deviations in the angular observable $P'_5(B \rightarrow K^* \mu^+ \mu^-)$ [3–7]. These discrepancies motivate scientists to conduct a diverse range of experiments to explore new aspects of physics and test the accuracy of current theories [8, 9].

*e-mail: yadavajaykumar286@gmail.com

**e-mail: manasmohapatra12@gmail.com

***e-mail: suchismita8792@gmail.com

In this work, we study the rare semileptonic decay channel, $B_c \rightarrow D_s^* \mu^+ \mu^-$ with the Effective Field Theory (EFT) formalism. This channel has been studied using various approaches such as the relativistic quark model (RQM)[10], QCD sum rules[11, 12], covariant confined quark model[13, 14] the light front quark model, and the constituent quark model along with specific NP model like Z' and Leptoquark[15] and in model independent approaches[16, 17]. Recently the LHCb Collaboration has established the upper limit for the $B_c \rightarrow D_s^* \mu^+ \mu^-$ channel, as well as the fragmentation fractions of B meson with c and u quarks at a 95% CL[18]. We fit the new coefficients by using the existing data on $b \rightarrow s \mu^+ \mu^-$ for both the 1D and 2D scenarios. We then examine the sensitivities of each scenarios for the branching ratio, forward backward asymmetry, lepton nonuniversality (LNU) parameter of $B_c \rightarrow D_s^* \mu^+ \mu^-$ decay mode.

The paper is structured in the following manner. In section 2, we delve into the theoretical framework of $B_c \rightarrow D_s^* \mu^+ \mu^-$ decay process in the EFT approach. We provide the global fit analysis for both the 1D and 2D scenarios of new Wilson coefficients in section 3. The discussion in section 4 includes the effects of the constrained new parameters on the various observable of the $B_c \rightarrow D_s^* \mu^+ \mu^-$ process. Section 5 encompasses the summary and conclusion.

2 Theoretical Framework

2.1 General Effective Hamiltonian

The most general effective Hamiltonian for the rare semileptonic decay $b \rightarrow sll$, can be written as[19],

$$\mathcal{H}_{\text{eff}} = -\frac{4G_F}{\sqrt{2}} V_{tb} V_{ts}^* \left[C_7^{\text{eff}} O_7 + C'_7 O'_7 + \sum_{i=9,10,P,S} ((C_i + C_i^{\text{NP}}) O_i + C'_i O'_i) \right], \quad (1)$$

where G_F is the Fermi constant, V_{ij} are the CKM matrix elements, $O_i^{(')}$ are the effective operators

$$\begin{aligned} O_7 &= \frac{e}{16\pi^2} m_b (\bar{s}\sigma_{\mu\nu} P_R b) F^{\mu\nu}, & O'_7 &= \frac{e}{16\pi^2} m_b (\bar{s}\sigma_{\mu\nu} P_L b) F^{\mu\nu} \\ O_9 &= \frac{e^2}{16\pi^2} (\bar{s}\gamma_\mu P_L b)(\bar{\mu}\gamma^\mu \mu), & O'_9 &= \frac{e^2}{16\pi^2} (\bar{s}\gamma_\mu P_R b)(\bar{\mu}\gamma^\mu \mu), \\ O_{10} &= \frac{e^2}{16\pi^2} (\bar{s}\gamma_\mu P_L b)(\bar{\mu}\gamma^\mu \gamma_5 \mu), & O'_{10} &= \frac{e^2}{16\pi^2} (\bar{s}\gamma_\mu P_R b)(\bar{\mu}\gamma^\mu \gamma_5 \mu), \\ O_S &= \frac{e^2}{16\pi^2} m_b (\bar{s}P_R b)(\bar{\mu}\mu), & O'_S &= \frac{e^2}{16\pi^2} m_b (\bar{s}P_L b)(\bar{\mu}\mu), \\ O_P &= \frac{e^2}{16\pi^2} m_b (\bar{s}P_R b)(\bar{\mu}\gamma_5 \mu), & O'_P &= \frac{e^2}{16\pi^2} m_b (\bar{s}P_L b)(\bar{\mu}\gamma_5 \mu), \end{aligned}$$

and $C_i^{(')}$ are corresponding Wilson coefficients. In the Standard Model, the primed coefficients are zero, but they can be nonzero in the presence of new physics. The coefficient C_9^{eff} includes a short-distance perturbative component, defined as:

$$C_9^{\text{eff}}(q^2) = C_9 + Y_{SD}(q^2) \quad (2)$$

where, the sort-distance contribution part is given as[20]

$$\begin{aligned}
Y_{SD}(q^2) &= h\left(\frac{m_c}{m_B}, q^2\right)(3C_1 + C_2 + 3C_3 + C_4 + 3C_5 + C_6) - \frac{1}{2}h(1, q^2)(4C_3 + 4C_4 + 3C_5 + C_6) \\
&\quad - \frac{1}{2}h(0, q^2)(C_3 + 3C_4) + \frac{2}{9}(3C_3 + C_4 + 3C_5 + C_6), \\
h(0, q^2) &= \frac{8}{27} - \ln \frac{m_b}{\mu} - \frac{4}{9} \ln s + \frac{4}{9}i\pi, \\
h(z, q^2) &= -\ln \frac{m_b}{\mu} - \frac{8}{9} \ln z + \frac{8}{27} \times \frac{4}{9} \times \frac{4z^2}{s} \\
&\quad - \frac{2}{9}\left(2 + \frac{4z^2}{s}\right)\sqrt{\left|1 - \frac{4z^2}{s}\right|} \begin{cases} \ln \left| \frac{\sqrt{1 - \frac{4z^2}{s}} + 1}{\sqrt{1 - \frac{4z^2}{s}} - 1} \right| - i\pi, & \text{for } \frac{4z^2}{s} < 1 \\ 2 \arctan \frac{1}{\sqrt{\frac{4z^2}{s} - 1}}, & \text{for } \frac{4z^2}{s} > 1 \end{cases}
\end{aligned}$$

with, $s = \frac{q^2}{m_B^2}$ and m_B is the mass of B meson.

2.2 $B_c \rightarrow D_s^* \mu^+ \mu^-$

Using the general effective Hamiltonian 1, the q^2 dependent differential branching ratio for the $B_c \rightarrow D_s^* \mu^+ \mu^-$ process is defined as

$$\frac{d\Gamma}{dq^2} = \frac{1}{4} [3I_1^c + 6I_1^s - I_2^c - 2I_2^s], \quad (3)$$

where $I_{1,2}^{c,s}$'s are the angular coefficients. Besides the differential decay distribution, we also scrutinize other physical observables such as forward-backward asymmetry A_{FB} , longitudinal (transverse) polarization fraction $F_{L(T)}$, form factor independent angular observables P'_4 , P'_5 and the lepton nonuniversality ratio. These observables are defined as[21–23] follows:

- **Forward-backward asymmetry:**

$$A_{FB}(q^2) = \frac{3I_6}{3I_1^c + 6I_1^s - I_2^c - 2I_2^s}. \quad (4)$$

- **Longitudinal and transverse polarization fractions:**

$$F_L(q^2) = \frac{3I_1^c - I_2^c}{3I_1^c + 6I_1^s - I_2^c - 2I_2^s}, \quad F_T(q^2) = 1 - F_L(q^2). \quad (5)$$

- **Lepton non-universality ratio:**

$$R_{D_s^*}(q^2) = \frac{d\Gamma(B_c \rightarrow D_s^* \mu^+ \mu^-)/dq^2}{d\Gamma(B_c \rightarrow D_s^* e^+ e^-)/dq^2}. \quad (6)$$

- **Form factor independent observable ($P'_{4,5}$):**

$$P'_4 = \frac{I_4}{\sqrt{-I_2^c I_2^s}}, \quad P'_5 = \frac{I_5}{2 \sqrt{-I_2^c I_2^s}}. \quad (7)$$

All the angular coefficients $I_i^{c,s}$'s ($i = 1, 2, \dots$) in terms of the transversity amplitudes and the transversity amplitudes as a functions of the form factors and Wilson coefficients are given in the appendix A.

3 Numerical Fits to the Model Parameters

This paper scrutinize the impact of (axial)vector coefficients on $B_c \rightarrow D_s^* \mu^+ \mu^-$ decay mode. To determine the best fit values of the (axial)vector coefficients $C_{9,10}^{(')NP}$, we perform a χ^2 fit of these coefficients to the existing data on $b \rightarrow s \mu^+ \mu^-$ observables using the flavio package [24]. We have used the following $b \rightarrow s \mu^+ \mu^-$ observables for our analysis.

- **Branching ratios:** Branching ratios of rare (semi)leptonic decay modes mediated by the $b \rightarrow s \mu^+ \mu^-$ transitions such as $B_s \rightarrow \mu^+ \mu^-$, $B^{+(0)} \rightarrow K^{+(0)} \mu^+ \mu^-$, $B^{+(0)} \rightarrow K^{*+(0)} \mu^+ \mu^-$ and $B_s \rightarrow \phi \mu^+ \mu^-$ in different q^2 bins.
- **Physical observables of $B_{(s)} \rightarrow K^*(\phi) \mu^+ \mu^-$:** Forward backward asymmetries, longitudinal polarization asymmetries, form factor independent observables, CP averaged angular observables, CP asymmetries in different q^2 bins.

We have taken two possible hypothesis: (a) only one Wilson coefficients at a time (1D) and (b) two Wilson coefficients at a time (2D). Fitting the above observables, the bestfit values, 1σ range, pull = $\sqrt{\chi_{\text{SM}}^2 - \chi_{\text{best-fit}}^2}$ values and the p-value (%) for the 1D scenarios are given in Table 1 and for the 2D scenarios are provided in Table 2. Table 1 shows that the pull value

Table 1. Best-fit values [1σ], pull and p values of different new physics scenarios of single coefficient.

Scenario	Coefficient	Best fit value [1σ]	Pull	p-value (%)
S - I	C_9^{NP}	-1.227 [-0.959, -1.363]	4.665	46.0
S - II	C_9^{NP}	0.456 [0.555, 0.252]	2.823	22.0
S - III	C_{10}^{NP}	0.082 [0.353, -0.252]	0.261	14.0
S - IV	C_{10}^{NP}	-0.134 [-0.050, -0.252]	1.085	13.0
S - V	$C_9^{\text{NP}} = C_{10}^{\text{NP}}$	0.023 [0.250, -0.050]	0.158	15.0
S - VI	$C_9^{\text{NP}} = -C_{10}^{\text{NP}}$	-0.971 [-0.757, -1.161]	4.921	53.0
S - VII	$C_9^{\text{NP}} = C_{10}^{\text{NP}}$	-0.135 [-0.052, -0.251]	1.003	14.0
S - VIII	$C_9^{\text{NP}} = -C_{10}^{\text{NP}}$	0.109 [0.147, 0.048]	1.046	15.0
S - IX	$C_9^{\text{NP}} = -C_9^{\text{NP}}$	-0.835 [-0.656, -0.959]	3.993	31.0
S - X	$C_9^{\text{NP}} = -C_{10}^{\text{NP}} = -C_9^{\text{NP}} = -C_{10}^{\text{NP}}$	-0.374 [-0.254, -0.451]	3.067	24.0
S - XI	$C_9^{\text{NP}} = -C_{10}^{\text{NP}} = C_9^{\text{NP}} = -C_{10}^{\text{NP}}$	-0.281 [-0.150, -0.454]	2.415	20.0

Table 2. Best-fit values [1σ], pull and p values of different new physics scenarios of two coefficients.

Scenario	Coefficient	Best fit value [1σ]	Pull	p-value (%)
S - I	$(C_9^{\text{NP}}, C_{10}^{\text{NP}})$	(-1.398[-1.219, -1.578], 0.694[0.855, 0.480])	5.961	67.0
S - II	$(C_9^{\text{NP}}, C_9^{\text{NP}})$	(-1.206[-0.988, -1.428], -0.053[-0.301, -0.386])	4.640	47.0
S - III	$(C_9^{\text{NP}}, C_{10}^{\text{NP}})$	(-1.269[-1.079, -1.454], -0.306[-0.158, -0.390])	5.239	53.0
S - IV	$(C_{10}^{\text{NP}}, C_9^{\text{NP}})$	(0.516[0.634, 0.291], -0.050[-0.333, -0.341])	3.106	16.0
S - V	$(C_{10}^{\text{NP}}, C_{10}^{\text{NP}})$	(0.469[0.680, 0.262], 0.101[0.237, -0.088])	2.565	20.0
S - VI	$(C_9^{\text{NP}}, C_{10}^{\text{NP}})$	(-0.033[-0.283, -0.379], -0.133[-0.008, -0.278])	1.059	13.0
S - VII	$(C_9^{\text{NP}} = -C_9^{\text{NP}}, C_{10}^{\text{NP}} = C_{10}^{\text{NP}})$	(-0.811[-0.636, -0.996], 0.128[0.273, -0.018])	3.689	36.0
S - VIII	$(C_9^{\text{NP}} = C_9^{\text{NP}}, C_{10}^{\text{NP}} = -C_{10}^{\text{NP}})$	(-1.121[-0.911, -1.330], 0.302[0.365, 0.198])	5.174	51.0
S - IX	$(C_9^{\text{NP}} = C_9^{\text{NP}}, C_{10}^{\text{NP}} = C_{10}^{\text{NP}})$	(-0.838[-1.077, -0.600], 0.015[-0.141, -0.172])	4.032	31.0
S - X	$(C_9^{\text{NP}} = -C_{10}^{\text{NP}}, C_9^{\text{NP}} = C_{10}^{\text{NP}})$	(-0.986[-0.783, -1.189], 0.108[0.232, -0.015])	5.412	53.0
S - XI	$(C_9^{\text{NP}} = -C_{10}^{\text{NP}}, C_9^{\text{NP}} = -C_{10}^{\text{NP}})$	(-1.008[-0.800, -1.217], -0.089[-0.033, -0.211])	4.922	49.0

for the S-VI ($C_9^{\text{NP}} = -C_{10}^{\text{NP}}$) scenario is largest among all possible 1D scenarios, followed by

the S - I (C_9^{NP}) scenario. This indicates that these two scenarios provide the best and most acceptable fits compared to the others. Similarly, the ($C_9^{\text{NP}}, C_{10}^{\text{NP}}$) combination of two Wilson coefficient has the maximum pull value = 5.961, followed by S - X ($C_9^{\text{NP}} = -C_{10}^{\text{NP}}, C_9^{\text{NP}} = C_{10}^{\text{NP}}$) scenario, S - III ($C_9^{\text{NP}}, C_{10}^{\text{NP}}$) and S - VIII ($C_9^{\text{NP}} = C_9^{\text{NP}}, C_{10}^{\text{NP}} = -C_{10}^{\text{NP}}$) scenario.

4 Results and Discussion

After collecting the best-fit values of all possible 1D and 2D scenarios of new coefficients, we now proceed to examine the sensitivity of these coefficients on the branching ratio and various angular observables of $B_c \rightarrow D_s^* \mu^+ \mu^-$ decay process. Using the best-fit values of all the 1D scenarios, the $q^2 \in [1, 6]$ variation of the branching ratio (top left), $R_{D_s^*}$ (top right), forward-backward asymmetry (middle left), longitudinal polarization asymmetry (middle right), P'_4 (bottom left) and P'_5 (bottom right) of $B_c \rightarrow D_s^* \mu^+ \mu^-$ decay mode is presented in the Fig. 1. In these figures, the black solid lines denote predictions from the Standard Model, while

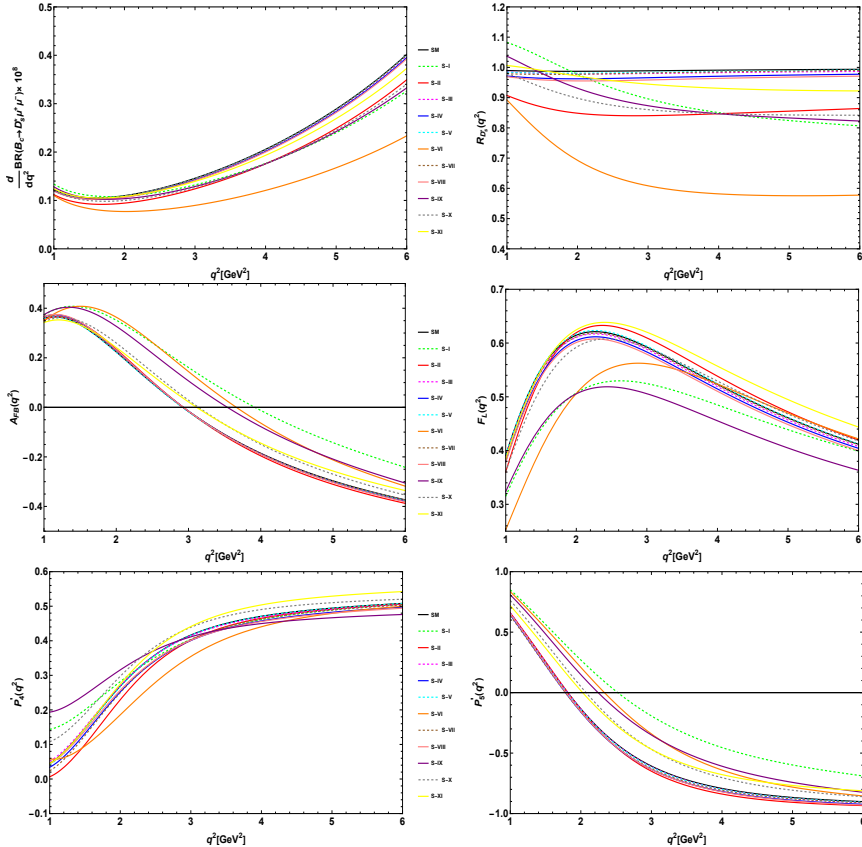


Figure 1. The $q^2 \in [1 - 6]$ behavior of branching ratio (top left), $R_{D_s^*}$ (top right), A_{FB} (middle left), F_L (middle right), P'_4 (bottom left) and P'_5 (bottom right) observables of $B_c \rightarrow D_s^* \mu^+ \mu^-$ with 1D scenarios. Here, the black solid lines represent the Standard Model predictions, while the solid and dashed lines of different colors represent results for various scenarios.

the colored solid and dashed lines represent results for various scenarios involving one co-

efficient. The branching ratio and other observables show the maximum deviation from the SM for the scenarios S-VI ($C_9^{\text{NP}} = -C_{10}^{\text{NP}}$) and S-I (C_9^{NP}). When only the new coefficient C_9^{NP} is present, the zero crossings of A_{FB} and P'_5 observables exhibit the greatest deviation. The predicted numerical values for $q^2 \in [1, 6]$ bin are provided in Table 3. Fig. 2 illus-

Table 3. Numerical predictions for observables of $B_c \rightarrow D_s^* \mu^+ \mu^-$ with 1D scenarios.

Scenarios	$BR \times 10^8$	$\langle R_{D_s^*} \rangle$	$\langle A_{FB} \rangle$	$\langle F_L \rangle$	$\langle P'_4 \rangle$	$\langle P'_5 \rangle$
SM	0.995909	0.990933	-0.15029	0.502247	0.43307	-0.665084
S - I	0.872324	0.867965	0.0141311	0.458742	0.425605	-0.324654
S - II	0.858233	0.853944	-0.157366	0.51103	0.421312	-0.697741
S - III	0.988079	0.983141	-0.151481	0.497999	0.430796	-0.67033
S - IV	0.976067	0.971119	-0.152712	0.493239	0.419947	-0.689361
S - V	0.991937	0.98698	-0.153195	0.503311	0.43277	-0.671721
S - VI	0.613327	0.610262	-0.0277296	0.47869	0.390046	-0.46957
S - VII	0.989827	0.984881	-0.151105	0.500223	0.423805	-0.681056
S - VIII	0.969369	0.964525	-0.15354	0.489112	0.41931	-0.691372
S - IX	0.865568	0.861242	-0.045553	0.433772	0.421539	-0.469868
S - X	0.863225	0.858911	-0.113459	0.502416	0.449859	-0.559257
S - XI	0.942656	0.937945	-0.11124	0.530621	0.458189	-0.545882

trates the impact of 2D scenarios on various observables for the decay $B_c \rightarrow D_s^* \mu^+ \mu^-$ with q^2 . The panels show the branching ratio (top left), $R_{D_s^*}$ (top right), forward-backward asymmetry (middle left), longitudinal polarization asymmetry (middle right), P'_4 (bottom left) and P'_5 (bottom right). The solid black lines represent SM results, while the colored solid and dashed lines depict predictions from various 2D scenarios. The deviation in almost all the observables are significant for S-I ($C_9^{\text{NP}}, C_{10}^{\text{NP}}$), S-X ($C_9^{\text{NP}} = -C_{10}^{\text{NP}}, C_9^{\text{NP}} = C_{10}^{\text{NP}}$) and S-XI ($C_9^{\text{NP}} = -C_{10}^{\text{NP}}, C_9^{\text{NP}} = -C_{10}^{\text{NP}}$) scenarios. Scenarios S-I and S-III induce the largest shifts in the zero crossings of the A_{FB} and P'_5 observables. The predicted numerical values for 2D scenarios are presented in Table 4.

Table 4. Numerical predictions for observables of $B_c \rightarrow D_s^* \mu^+ \mu^-$ with 2D scenarios.

Scenario	$BR \times 10^8$	$\langle R_{D_s^*} \rangle$	$\langle A_{FB} \rangle$	$\langle F_L \rangle$	$\langle P'_4 \rangle$	$\langle P'_5 \rangle$
SM	0.995909	0.990933	-0.15029	0.502247	0.43307	-0.665084
S - I	0.659425	0.65613	0.0450635	0.452897	0.400632	-0.298963
S - II	0.876757	0.872375	0.0108972	0.461804	0.425682	-0.33026
S - III	0.826409	0.822279	0.0233328	0.430211	0.392443	-0.358219
S - IV	0.846171	0.841942	-0.157336	0.515268	0.421405	-0.697981
S - V	0.868733	0.864392	-0.15552	0.517975	0.431423	-0.678396
S - VI	0.979493	0.974599	-0.152309	0.495055	0.421005	-0.687147
S - VII	0.846813	0.842581	-0.0530879	0.446196	0.430432	-0.470705
S - VIII	0.858104	0.853815	-0.0113529	0.489383	0.395102	-0.397493
S - IX	0.981172	0.976268	-0.0393625	0.509791	0.43836	-0.406841
S - X	0.615151	0.612077	-0.026341	0.480789	0.401619	-0.447669
S - XI	0.618286	0.615196	-0.0213378	0.490384	0.400763	-0.434288

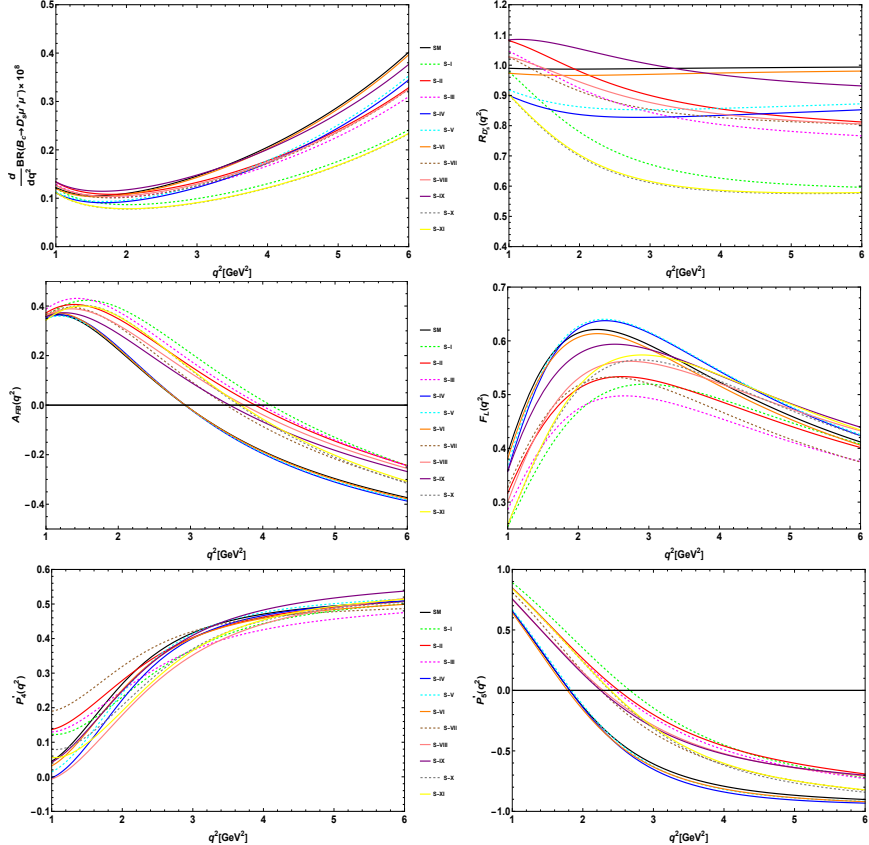


Figure 2. The q^2 behavior of branching ratio (top left), $R_{D_s^*}$ (top right), A_{FB} (middle left), F_L (middle right), P'_4 (bottom left) and P'_5 (bottom right) observables of $B_c \rightarrow D_s^* \mu^+ \mu^-$ with 2D scenarios. The black solid lines represent Standard Model predictions, while the colored solid and dashed lines denote results for various scenarios.

5 Conclusion

In this work, we studied the $B_c \rightarrow D_s^* \mu^+ \mu^-$ decay mode using an Effective Field Theory approach, considering cases with either one (1D) or two (2D) unknown Wilson coefficients associated with (axial)vector operators. We performed a global fit analysis of these new Wilson coefficients using existing experimental data on $b \rightarrow s \mu^+ \mu^-$ observables. Based on the best-fit values from both 1D and 2D scenarios, we estimated the branching ratio and various angular observables for $B_c \rightarrow D_s^* \mu^+ \mu^-$ process in the q^2 range [1, 6] GeV^2 . These observables include forward-backward asymmetry, longitudinal polarization asymmetry, form factor-independent observables, and lepton nonuniversality parameter. We observed significant deviations from the Standard Model predictions, particularly for the scenarios with only C_9^{NP} and $C_9^{\text{NP}} = -C_{10}^{\text{NP}}$ in the 1D case, and for the 2D scenarios: $(C_9^{\text{NP}}, C_{10}^{\text{NP}})$, $(C_9^{\text{NP}} = -C_{10}^{\text{NP}}, C_9^{\text{NP}} = C_{10}^{\text{NP}})$ and $(C_9^{\text{NP}} = -C_{10}^{\text{NP}}, C_9^{\text{NP}} = -C_{10}^{\text{NP}})$. This analysis suggests the need for a thorough experimental investigation of the rare semileptonic decay $B_c \rightarrow D_s^* \mu^+ \mu^-$ in the near future.

Acknowledgment

AKY expresses gratitude to the DST-Inspire Fellowship division, Government of India, for financial support under ID No. IF210687. MKM would like to acknowledge financial support from the IoE PDRF at the University of Hyderabad.

A The angular coefficients I_i

The angular coefficients I_i as a functions of the transversity amplitudes are defined as [21, 25, 26],

$$\begin{aligned}
I_1^c &= \left(|A_L^0|^2 + |A_R^0|^2\right) + 8 \frac{m_l^2}{q^2} \text{Re}\left[A_L^0 A_R^{0*}\right] + 4 \frac{m_l^2}{q^2} |A_t|^2, \\
I_2^c &= -\beta_l^2 \left(|A_L^0|^2 + |A_R^0|^2\right), \\
I_1^s &= \frac{(2 + \beta_l^2)}{4} \left[|A_L^\perp|^2 + |A_L^\parallel|^2 + |A_R^\perp|^2 + |A_R^\parallel|^2\right] + \frac{4 m_l^2}{q^2} \text{Re}\left[A_L^\perp A_R^{\perp*} + A_L^\parallel A_R^{\parallel*}\right], \\
I_2^s &= \frac{1}{4} \beta_l^2 \left[|A_L^\perp|^2 + |A_L^\parallel|^2 + |A_R^\perp|^2 + |A_R^\parallel|^2\right], \\
I_3 &= \frac{1}{2} \beta_l^2 \left[|A_L^\perp|^2 - |A_L^\parallel|^2 + |A_R^\perp|^2 - |A_R^\parallel|^2\right], \\
I_4 &= \frac{1}{\sqrt{2}} \beta_l^2 \left[\text{Re}\left(A_L^0 A_L^{\parallel*}\right) + \text{Re}\left(A_R^0 A_R^{\parallel*}\right)\right], \\
I_5 &= \sqrt{2} \beta_l \left[\text{Re}\left(A_L^0 A_L^{\perp*}\right) - \text{Re}\left(A_R^0 A_R^{\perp*}\right)\right],
\end{aligned}$$

where the transversity amplitude, $A_{R,L}^{\perp,\parallel,0}$ in terms of form factors are given by

$$\begin{aligned}
A_{R,L}^0 &= -N_{D_s^*} \frac{1}{2 m_{D_s^*} \sqrt{q^2}} \left[(C_9^{eff} \pm C_{10}) \left[(m_{B_s}^2 - m_{D_s^*}^2 - q^2)(m_{B_s} + m_{D_s^*}) A_1 - \frac{\lambda(m_{B_c}^2, m_{D_s^*}^2, q^2)}{m_{B_s} + m_{D_s^*}} A_2 \right] \right. \\
&\quad \left. + 2 m_b C_7^{eff} \left[(m_{B_s}^2, +3 m_{D_s^*}^2, -q^2) T_2 - \frac{\lambda(m_{B_c}^2, m_{D_s^*}^2, q^2)}{m_{B_s}^2 - m_{D_s^*}^2} T_3 \right] \right], \\
A_{R,L}^\perp &= N_{D_s^*} \sqrt{2} \left[(C_9^{eff} \pm C_{10}) \frac{\sqrt{\lambda(m_{B_c}^2, m_{D_s^*}^2, q^2)}}{m_{B_s} + m_{D_s^*}} V + \frac{\sqrt{\lambda(m_{B_c}^2, m_{D_s^*}^2, q^2)} 2 m_b C_7^{eff}}{q^2} T_1 \right], \\
A_{R,L}^\parallel &= -N_{D_s^*} \sqrt{2} \left[(C_9^{eff} \pm C_{10})(m_{B_s} + m_{D_s^*}) A_1 + \frac{2 m_b C_7^{eff} (m_{B_s}^2 - m_{D_s^*}^2)}{q^2} T_2 \right], \\
A_{R,L}^t &= 2 N_{D_s^*} C_{10} \frac{\sqrt{\lambda(m_{B_c}^2, m_{D_s^*}^2, q^2)}}{\sqrt{q^2}} A_0,
\end{aligned}$$

with

$$N_{D_s^*} = \left[\frac{G_F^2 \alpha_e^2}{3.2^{10} \pi^5 m_{B_s}^3} |V_{tb} V_{ts}^*|^2 q^2 \sqrt{\lambda(m_{B_c}^2, m_{D_s^*}^2, q^2)} \left(1 - \frac{4 m_l^2}{q^2}\right)^{1/2} \right]^{1/2}.$$

References

- [1] A. Seuthe (LHCb), Lepton flavour universality tests at LHCb, in *57th Rencontres de Moriond on QCD and High Energy Interactions* (2023), 2305.08216

- [2] R. Aaij et al. (LHCb), Measurement of lepton universality parameters in $B^+ \rightarrow K^+\ell^+\ell^-$ and $B^0 \rightarrow K^{*0}\ell^+\ell^-$ decays, Phys. Rev. D **108**, 032002 (2023), [2212.09153](#). [10.1103/PhysRevD.108.032002](#)
- [3] A.J. Buras, Standard Model predictions for rare K and B decays without new physics infection, Eur. Phys. J. C **83**, 66 (2023), [2209.03968](#). [10.1140/epjc/s10052-023-11222-6](#)
- [4] A.M. Sirunyan et al. (CMS), Measurement of angular parameters from the decay $B^0 \rightarrow K^{*0}\mu^+\mu^-$ in proton-proton collisions at $\sqrt{s} = 8$ TeV, Phys. Lett. B **781**, 517 (2018), [1710.02846](#). [10.1016/j.physletb.2018.04.030](#)
- [5] R. Aaij et al. (LHCb), Angular Analysis of the $B^+ \rightarrow K^{*+}\mu^+\mu^-$ Decay, Phys. Rev. Lett. **126**, 161802 (2021), [2012.13241](#). [10.1103/PhysRevLett.126.161802](#)
- [6] R. Aaij et al. (LHCb), Measurement of CP -Averaged Observables in the $B^0 \rightarrow K^{*0}\mu^+\mu^-$ Decay, Phys. Rev. Lett. **125**, 011802 (2020), [2003.04831](#). [10.1103/PhysRevLett.125.011802](#)
- [7] M. Algueró, A. Biswas, B. Capdevila, S. Descotes-Genon, J. Matias, M. Novo-Brunet, To (b)e or not to (b)e: no electrons at LHCb, Eur. Phys. J. C **83**, 648 (2023), [2304.07330](#). [10.1140/epjc/s10052-023-11824-0](#)
- [8] J. Woithe, G.J. Wiener, F.F. Van der Veken, Let's have a coffee with the Standard Model of particle physics!, Phys. Educ. **52**, 034001 (2017). [10.1088/1361-6552/aa5b25](#)
- [9] D. Saikumar, Exploring the Frontiers: Challenges and Theories Beyond the Standard Model (2024), [2404.03666](#).
- [10] D. Ebert, R.N. Faustov, V.O. Galkin, Rare Semileptonic Decays of B and B_c Mesons in the Relativistic Quark Model, Phys. Rev. D **82**, 034032 (2010), [1006.4231](#). [10.1103/PhysRevD.82.034032](#)
- [11] K. Azizi, F. Falahati, V. Bashiry, S.M. Zebarjad, Analysis of the Rare $B(c) \rightarrow D^*(s,d)$ $l+ l-$ Decays in QCD, Phys. Rev. D **77**, 114024 (2008), [0806.0583](#). [10.1103/PhysRevD.77.114024](#)
- [12] K. Azizi, R. Khosravi, Analysis of the rare semileptonic $B_c \rightarrow P(D, D_s)\ell^+\ell^-/\nu\bar{\nu}$ decays within QCD sum rules, Phys. Rev. D **78**, 036005 (2008), [0806.0590](#). [10.1103/PhysRevD.78.036005](#)
- [13] M.A. Ivanov, J.G. Körner, J.N. Pandya, P. Santorelli, N.R. Soni, C.T. Tran, Exclusive semileptonic decays of D and D_s mesons in the covariant confining quark model, Front. Phys. (Beijing) **14**, 64401 (2019), [1904.07740](#). [10.1007/s11467-019-0908-1](#)
- [14] M.A. Ivanov, J.N. Pandya, P. Santorelli, N.R. Soni, Decay $B_c^+ \rightarrow D_{(s)}^{(*)+}\ell^+\ell^-$ within covariant confined quark model (2024), [2404.15085](#).
- [15] M.K. Mohapatra, N. Rajeev, R. Dutta, Combined analysis of $Bc \rightarrow Ds^{(*)}\mu^+\mu^-$ and $Bc \rightarrow Ds^{(*)}\nu\bar{\nu}$ decays within Z' and leptoquark new physics models, Phys. Rev. D **105**, 115022 (2022), [2108.10106](#). [10.1103/PhysRevD.105.115022](#)
- [16] R. Dutta, Model independent analysis of new physics effects on $B_c \rightarrow (D_s, D_s^*)\mu^+\mu^-$ decay observables, Phys. Rev. D **100**, 075025 (2019), [1906.02412](#). [10.1103/PhysRevD.100.075025](#)
- [17] Y.S. Li, X. Liu, Angular distribution of the FCNC process $Bc \rightarrow Ds^*(\rightarrow Ds\pi)\ell^+\ell^-$, Phys. Rev. D **108**, 093005 (2023), [2309.08191](#). [10.1103/PhysRevD.108.093005](#)
- [18] R. Aaij et al. (LHCb), A search for rare $B \rightarrow D\mu^+\mu^-$ decays, JHEP **02**, 032 (2024), [2308.06162](#). [10.1007/JHEP02\(2024\)032](#)
- [19] A. Ahmed, I. Ahmed, M.A. Paracha, M. Junaid, A. Rehman, M.J. Aslam, Comparative Study of $B_c \rightarrow D_s^*\ell^+\ell^-$ Decays in Standard Model and Supersymmetric Models (2011), [1108.1058](#)

- [20] A. Ali, P. Ball, L.T. Handoko, G. Hiller, A Comparative study of the decays $B \rightarrow (K, K^*)\ell^+\ell^-$ in standard model and supersymmetric theories, Phys. Rev. D **61**, 074024 (2000), hep-ph/9910221. [10.1103/PhysRevD.61.074024](https://doi.org/10.1103/PhysRevD.61.074024)
- [21] W. Altmannshofer, P. Ball, A. Bharucha, A.J. Buras, D.M. Straub, M. Wick, Symmetries and Asymmetries of $B \rightarrow K^*\mu^+\mu^-$ Decays in the Standard Model and Beyond, JHEP **01**, 019 (2009), 0811.1214. [10.1088/1126-6708/2009/01/019](https://doi.org/10.1088/1126-6708/2009/01/019)
- [22] J. Matias, F. Mescia, M. Ramon, J. Virto, Complete Anatomy of $\bar{B}_d -> \bar{K}^{*0}(- > K\pi)l^+l^-$ and its angular distribution, JHEP **04**, 104 (2012), 1202.4266. [10.1007/JHEP04\(2012\)104](https://doi.org/10.1007/JHEP04(2012)104)
- [23] S. Sahoo, R. Mohanta, Study of the rare semileptonic decays $B_d^0 \rightarrow K^*l^+l^-$ in scalar leptoquark model, Phys. Rev. D **93**, 034018 (2016), 1507.02070. [10.1103/PhysRevD.93.034018](https://doi.org/10.1103/PhysRevD.93.034018)
- [24] D.M. Straub, flavio: a Python package for flavour and precision phenomenology in the Standard Model and beyond (2018), 1810.08132.
- [25] C. Bobeth, G. Hiller and G. Piranishvili, JHEP **07** (2008), 106 doi:10.1088/1126-6708/2008/07/106 [arXiv:0805.2525 [hep-ph]].
- [26] F. Kruger, J. Matias, Probing new physics via the transverse amplitudes of $B^0 \rightarrow K^{*0}(\rightarrow K^-\pi^+)l^+l^-$ at large recoil, Phys. Rev. D **71**, 094009 (2005), hep-ph/0502060. [10.1103/PhysRevD.71.094009](https://doi.org/10.1103/PhysRevD.71.094009)